

Linear HgCdTe radiometer

G. Eppeldauer and L. Novak[†]

Radiometric Physics Division, National Institute of Standards and Technology, Gaithersburg, Maryland 20899

ABSTRACT

The basic modes of electrical operation of photoconductive optical radiation detectors are analyzed. The nonlinearity inherent in "voltage mode" measurements can be eliminated by using "current mode" measurements. A HgCdTe photoconductive radiometer has been designed, based on this analysis, which measures the current through a biased detector. A built-in calibrating capability in the circuits of the radiometer makes it possible to eliminate the effects of a long-term drift in the bias voltage, thereby achieving a higher precision.

1. INTRODUCTION

Photoconductors exhibit a change in conductance (the inverse of resistance) when radiant power is applied to them. In order to sense the photogenerated conductance change, the photoconductor is operated with a bias current. A traditional biasing circuit¹ consists of a DC source and a load resistor, as shown later in Fig. 1. Manufacturers often recommend measurement of the voltage change across the detector while passing a constant current through it²⁻⁴.

These practices give an output voltage that is a nonlinear function of the conductance change. The conductance change, to a good approximation, is proportional to the incident flux on the detector⁵. In multidecade radiant power measurements, the nonlinear response of the detector circuit introduces unwanted errors. In order to eliminate them, either the nonlinearity has to be electrically compensated using additional circuits⁶ or an inherently linear circuit has to be used. The latter solution promises higher accuracy and simpler implementation. Therefore, we proceed to analyze the different ways a photoconductor can be used in a circuit, with a goal of designing a photoconductive radiometer which has an output signal proportional to the conductance change of the detector. This kind of design can be used more accurately for radiometric measurements over a wide dynamic range.

2. MODES OF ELECTRICAL OPERATION

2.1. Voltage mode measurements

A basic photoconductive detector biasing and measuring circuit is shown in Fig. 1. A steady voltage source V_B produces a biasing current I_B through the serially connected detector resistance R_D and load resistance R_L .

$$V_B = I_B (R_L + R_D) \quad (1)$$

The voltage across the load resistance is formed by the bias current,

$$V_L = I_B R_L \quad (2)$$

From Eqs. 1 and 2, V_L depends on the detector resistance R_D as:

$$V_L(R_D) = V_B \frac{R_L}{(R_L + R_D)} \quad (3)$$

As the detector resistance R_D is the reciprocal of its conductance, σ_D ,

$$R_D = \frac{1}{\sigma_D} \quad (4)$$

V_L depends upon the conductivity σ_D as:

$$V_L(\sigma_D) = V_B \frac{R_L \sigma_D}{(1 + R_L \sigma_D)} \quad (5)$$

[†] Present Address: Czechoslovak Academy of Sciences, Prague, Czechoslovakia

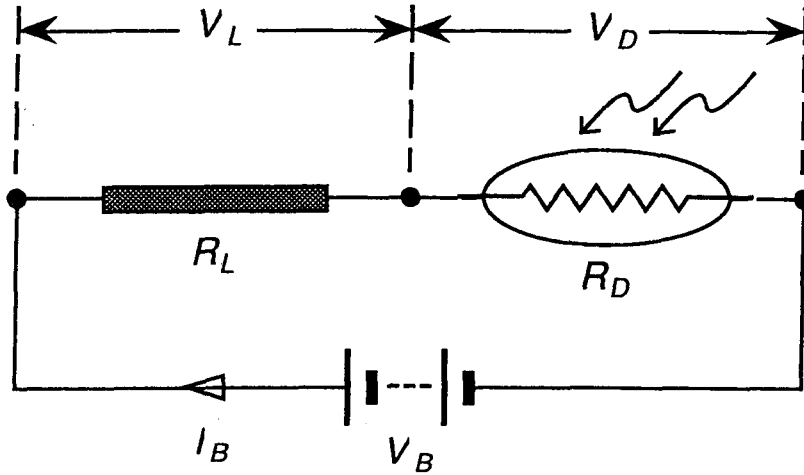


FIGURE 1: Voltage Mode

Eq. 5 shows that the output voltage on the load resistance is a nonlinear function of the detector conductance. Further, the relative magnitudes of R_L and R_D affect the measurement.

$$\text{When } R_L \gg R_D, \quad V_L \cong V_B \quad (6)$$

$$\text{When } R_L \ll R_D, \quad V_L \cong V_B R_L \sigma_D \quad (7)$$

In the first case, the output signal is insensitive to changes in σ_D . In the second, there is a linear approximation at the expense of signal strength ($R_L \sigma_D \ll 1$). All told, measuring V_L to determine changes in σ_D (as when optical radiation is measured) leads to inaccuracies.

Alternatively, one can derive an output signal by measuring the voltage across the detector,

$$V_D = I_B R_D \quad (8)$$

From Eqs. 1 and 8, we can express the detector voltage as a function of the detector resistance,

$$V_D(R_D) = V_B \frac{R_D}{(R_L + R_D)} \quad (9)$$

and as function of detector conductance:

$$V_D(\sigma_D) = V_B \frac{1}{(1 + R_L \sigma_D)} \quad (10)$$

Eq. 10 shows that again the voltage measurement is a nonlinear function of the detector conductance. Proceeding as before,

$$\text{When } R_L \ll R_D, \quad V_D \cong V_B \quad (11)$$

$$\text{When } R_L \gg R_D, \quad V_D \cong I_B / \sigma_D \quad (12)$$

Neither of these conditions are attractive. In the first, the output voltage is again insensitive to changes in detector conductance. In the other, where V_B and R_L act to form a constant current source I_B , the response is inversely proportional to the detector conductance. Both situations may lead to measurement errors when changes in V_D are presumed to be proportional to changes in σ_D .

2.2. Current mode measurements

Another basic photoconductive detector biasing and measuring circuit is shown in Fig. 2.

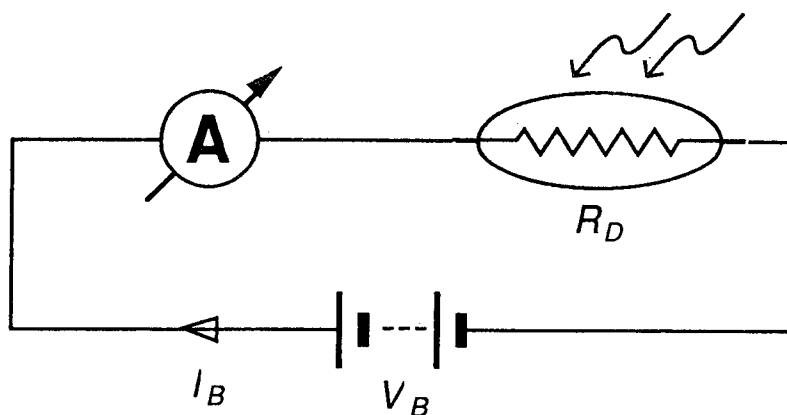


FIGURE 2: Current Mode

A current meter A measures the “short circuit current” of V_B and R_D treated together as a Thévenin voltage source, and is the limiting case of the previous circuit as R_L (and V_L) $\rightarrow 0$

$$I_B(\sigma_D) = V_B \sigma_D \quad (13)$$

This current, rather than a voltage, is linearly proportional to the detector conductance. For conductance changes (as when optical radiation is detected) it can be written

$$I_B = V_B (\sigma_D + \Delta\sigma_D) \quad (14)$$

or as:

$$I_B = I_B^0 + V_B \Delta\sigma_D \quad (15)$$

We see that there is both a constant biasing current, I_B^0 , and a “useful” current component which is proportional to the conductance change and to the biasing voltage. This part is generally the small difference of two large numbers, I_B and I_B^0 . To achieve high accuracy, the biasing voltage has to be very stable. Its internal resistance, as well as the internal resistance of the current meter, has to be much smaller than the detector resistance in order to satisfy the assumptions of this derivation.

3. ELECTRONIC DESIGN

A large-area (2.54 mm \times 2.54 mm) InfraRed Associates² HgCdTe (MCT) detector was selected for radiometric applications. The resistance range of large-area MCT detectors is roughly 15 to 30 ohm at 77 K. The selected one had a resistance of 24.7 ohm at this temperature. If we consider that the maximum resistance change of the detector for maximum optical radiation of 50 mW is about 10%, it follows that a 25 Ω detector will have a resistance change of about 25 $\mu\Omega$ if a radiant power level of 0.5 μ W has to be measured.

An amplifier unit was matched to the detector by the manufacturer, working on the principles analyzed in Section 2.1. This circuit operated in the voltage mode, where the voltage on the detector resistance was measured. In order to get the maximum signal to noise ratio, the detector required a bias current of 70 mA. If the detector was to be used with a customer’s bias circuitry and amplifier system, they suggested a serial load resistor ten times higher than the detector resistance. This corresponds to the nonlinear connection between the detector voltage and conductance described in Eq. 12.

In addition to the manufacturer’s amplifier unit, we developed another amplifier that made a current mode measurement, following the analysis in Section 2.2. It was based on an operational amplifier in the standard configuration to measure short-circuit current at the input, and it included provisions for biasing the detector. However, the bias current would have produced an unwanted, amplified output voltage, which in most cases would have saturated the amplifier. To avoid this, a voltage compensation method was used, as shown in Fig. 3.

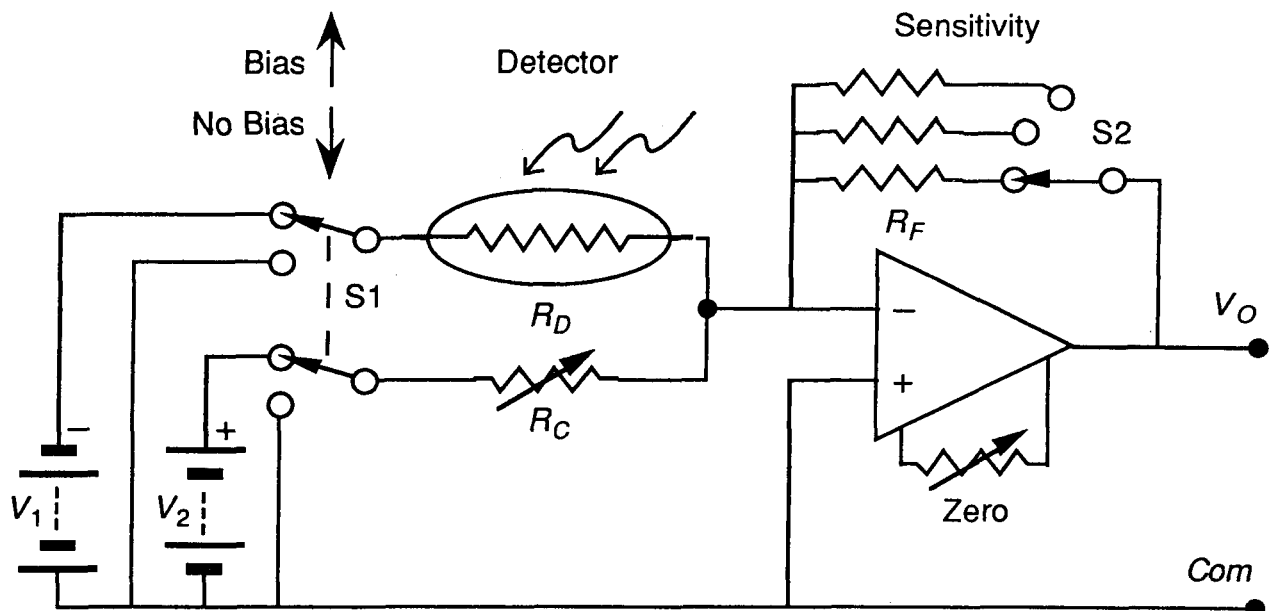


FIGURE 3: Current to Voltage Converter, Simplified Model

Voltage source V_1 is used to bias the detector and corresponds to V_B in the previous discussion. A compensating voltage V_2 , of opposite polarity, couples to the summation point of the operational amplifier through a variable resistor, R_C . When switch S1 is in the "No Bias" position, the voltage sources are removed from the circuit and the amplifier can be zeroed. When S1 is in the "Bias" position, R_C is adjusted for a null output ($V_O = 0$) when the detector is in the dark. Both of these adjustments should be performed at the highest amplifier gain (largest value of R_F) used for subsequent measurements. Once they are made, the output of the amplifier circuit

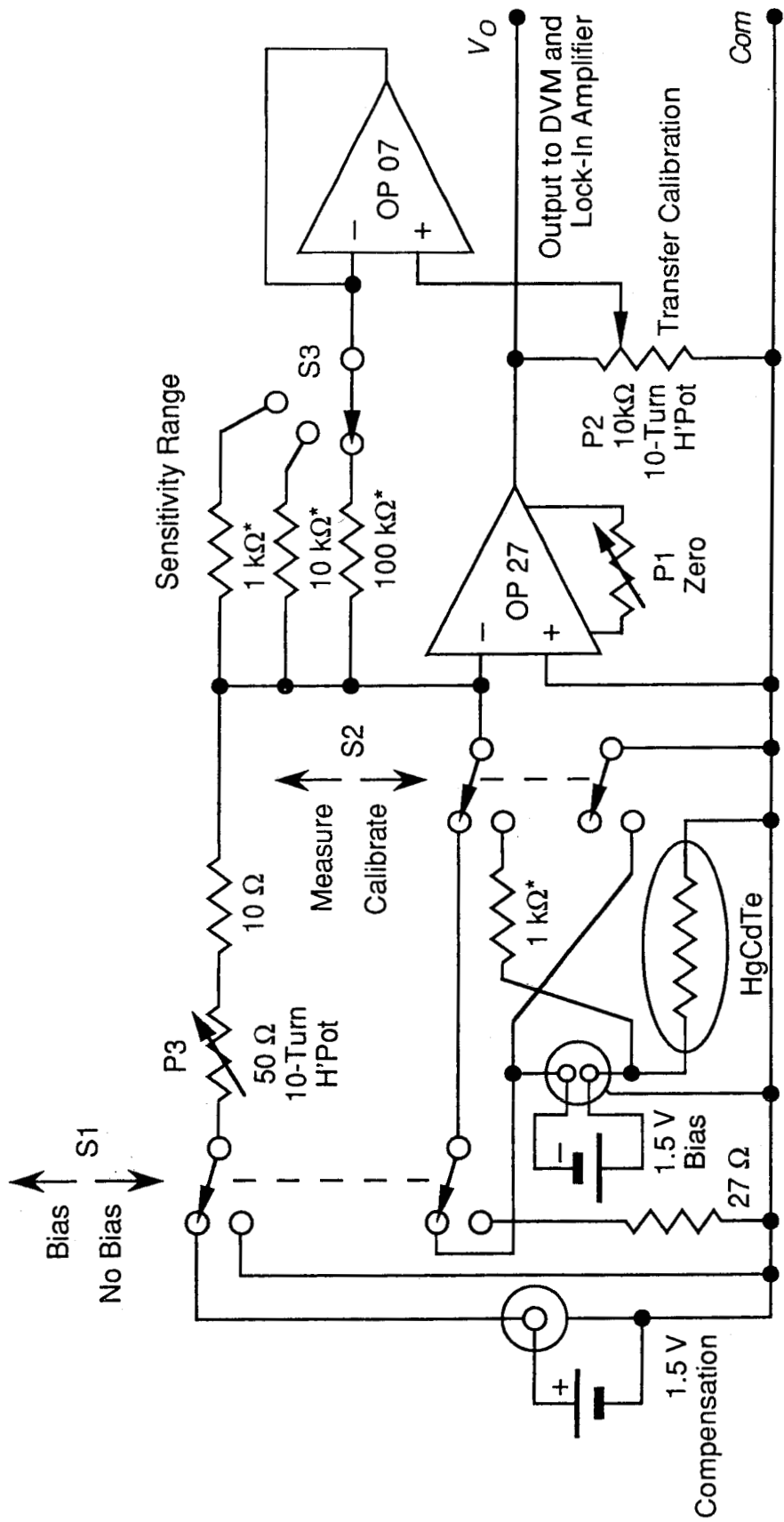
$$V_O = V_1 R_F \Delta\sigma_D \quad (16)$$

To make a useful circuit, it is necessary to do the compensation carefully. The voltage sources should be very stable and have low output impedances. The zero adjustments should be checked repeatedly to counteract changes of the voltage sources and resistors. Because of the high amplification required to detect small changes in σ_D , the circuit should be well shielded and grounded to minimize interference at the output. Additionally, the operational amplifier must have low noise, low drift, a large gain-bandwidth product, and a large open-loop gain. The gain of the amplifier should be calibrated repeatedly to make sure that the optical radiation measurements stay consistent over time.

Our actual amplifier circuit had additional features to allow us to make these gain calibrations. A diagram of the complete circuit is shown in Fig. 4. When switch S2 is in the up position, this circuit is similar to the one shown in Fig. 3. However, when switch S2 is in the down position, two changes are made. First, the negative terminal of the bias source is connected to a real ground, rather than the virtual ground at the summation point of the operational amplifier. This maintains the detector as a load across the bias voltage. Secondly, the operational amplifier is connected to measure the bias voltage itself, through a 1000 Ω resistor. If the bias voltage changes, so does the proportionality factor shown in Eq. 16. To counteract this change, the effective feedback resistance R_F can be changed with potentiometer P2 such that the transfer gain of the amplifier remains constant. Potentiometer P2 is followed by a buffer amplifier to maintain a uniform output impedance.

To summarize, the adjustment procedure is to:

- 1) Switch S1 to "No Bias", S2 to "Measure", turn S3, the Sensitivity Range, to the highest scale (the 100 k Ω resistor), and set P1 for zero output voltage.
- 2) Leave S1 on "No Bias", switch S2 to "Calibrate", change the Sensitivity Range to the lowest scale (the 1000 Ω resistor), and adjust P2 for a -1.990 ± 0.002 V output voltage while the detector is in the dark.
- 3) Change S1 to "Bias" and S2 to "Measure", return the Sensitivity Range to the highest scale, and adjust P3 for a null (zero) output voltage while the detector is in the dark.



*Precision Resistor

FIGURE 4: Current to Voltage Converter, Working Model

For biasing and compensation, we used with equal success both high charge-capacity alkaline batteries and electronically controlled, highly stable, ripple and noise free DC calibrators. If a battery is used as a biasing voltage source (it has minimum noise and ripple), the 70 mA load current may cause a long-term decrease in its output voltage. While the calibration of the amplifier transfer gain gives stability to the measuring circuit, it does not eliminate the bias-current dependent change in the detector responsivity. When a battery is used for biasing, the small changes in the bias voltage must be regarded as a potential source of error, which can be estimated using data provided by the detector manufacturer.

There is one more electronic detail concerning the measurement of optical radiation. In practice, the signal on the photodetector is chopped. The output of the amplifier circuit is detected by a "Lock-In Amplifier," which provides greater noise rejection than would a DC measurement, alone. Care must be taken that the amplifier has a sufficient bandwidth. In Fig. 5, we show a block diagram of the electronic instrumentation used for our measurements.

4. STABILITY

The use of this circuit for detector studies is beyond the scope of this paper. However, we would like to report that the radiometer operated stably over an extended period of time.

A tungsten strip lamp, fed from a highly stable DC current source and operating at about 100 °C, was imaged onto the MCT detector using a spherical mirror and an aperture 2 mm in diameter. The radiation was chopped at 13 Hz. The roll-off frequency of the low pass filter on the lock-in amplifier was set two decades lower. The sensitivity of the current to voltage converter was 10^5 Volts/Amp (the 100 k Ω feedback resistor).

Over the course of 122 minutes, 1269 voltage measurements were made at the output of the lock-in amplifier. These voltages held in the range between 9.078 and 9.173, with an average of 9.132. The standard deviation was 0.017 V, which corresponds to 0.19%.

Fig. 6 shows what happened after this data was taken. As the quantity of liquid nitrogen decreased in the dewer, the detector resistance changed, causing the compensation voltage and the bias voltage to be out of balance. However, when the dewer was refilled and the electronic adjustment procedure followed, the output readings matched the previous ones.

5. ACKNOWLEDGEMENTS

The authors thank Robert D. Saunders for participating in the stability measurements and Jonathan E. Hardis for help in preparing the manuscript.

6. REFERENCES

1. E. L. Dereniak and D. G. Crowe, *Optical Radiation Detectors*, p. 94, John Wiley & Sons (1984).
2. Commercial products – materials and instruments – are identified in this document for the sole purpose of adequately describing experimental or test procedures. In no event does such identification imply recommendation or endorsement by the National Institute of Standards and Technology of a particular product, nor does it imply that a named material or instrument is necessarily the best available for the purpose it serves.
3. *Infrared Components Brochure*, Edition 17, p. 58, Santa Barbara Research Center, Goleta, CA (1983).
4. *Technical Data Book, HgCdTe Instruction Manual*, p. 2, InfraRed Associates, Inc., Cranberry, NJ (1985).
5. E. L. Dereniak and D. G. Crowe, *ibid.*, p. 92.
6. *Linear and Conversion Applications Handbook*, pp. 240-241, Precision Monolithics, Inc., Santa Clara, CA (1986).

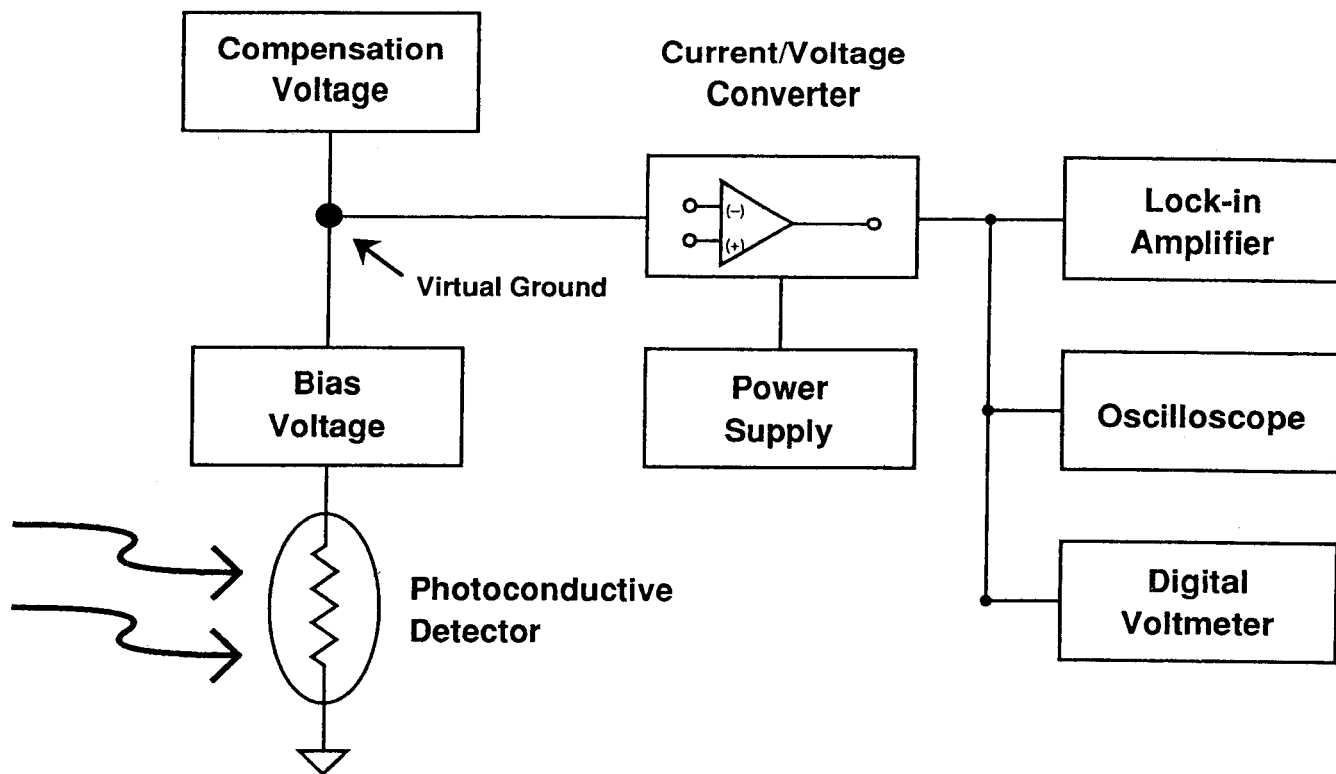


FIGURE 5: Block Diagram of Photoconductive Detector Radiometer

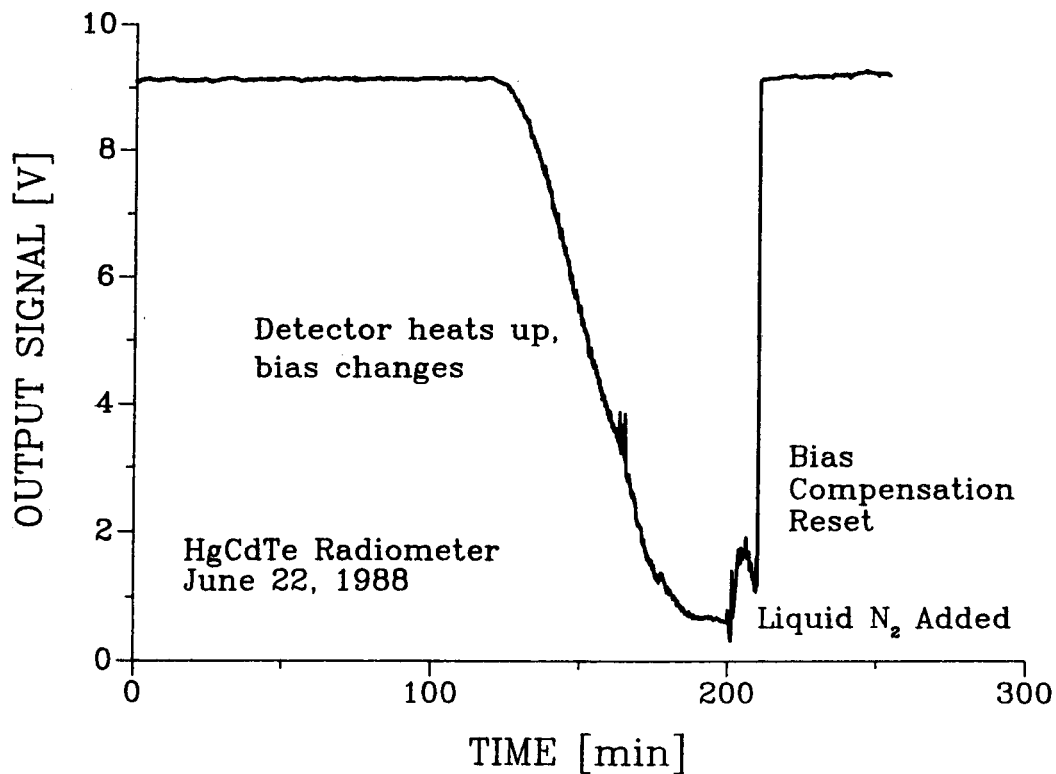


FIGURE 6: Detector Stability